Austin Egbert, Charles Baylis, Anthony Martone & Robert J. Marks
``Recursive Interval-Halving Method for Generating Model Independent Impedance Tuner Characterizations"
2021 IEEE Texas Symposium on Wireless and Microwave Circuits and Systems (WMCS), July 27, 2021, Waco, TX

2021 IEEE Texas Symposium on Wireless and Microwave Circuits and Systems (WMCS) | 978-1-6654-0309-2/21/$31.00 ©2021 IEEE | DOI: 10.1109/WMCS52222.2021.9493222

Recursive Interval-Halving Method for Generating Model Independent Impedance Tuner Characterizations

Austin Egbert[1], Charles Baylis[1], Anthony Martone[2], and Robert J. Marks II[1]

[1]Baylor University, Waco, Texas 76796, USA
[2]Army Research Laboratory, Adelphi, Maryland 20783, USA

***Abstract* — Existing impedance tuners are often able to utilize characterization processes that model the underlying behavior of the tuner's fundamental parameters to efficiently select a range of parameter settings that evenly span the device's potential impedance characteristics. However, new tuner implementations cannot take advantage of these processes without preestablished knowledge of their underlying behavior, and this behavior can be difficult to efficiently and reliably model. In such circumstances, a model-less characterization process is required to determine the device settings needed to span its possible impedance values efficiently and evenly. Here, a process using a recursive interval-halving approach is demonstrated for characterizing impedance tuners without the use of a model.**

***Index Terms* — automated impedance tuner, calibration, device characterization, load pull**

I. Introduction

Much effort has been expended into the development of real-time configurable and optimizable RF transmitter and receiver systems. One requirement for such a system is the ability to alter the impedances presented to the system's amplifiers. Traditional load pull impedance tuners are too slow for real-time operation and too large for integration into a final deployable system. In their place, various reconfigurable impedance tuners have been designed that are able to adapt faster and are housed in a much smaller package.

Although such newer technologies may not require the use of a characterization when used to optimize an amplifier system [1], it is nevertheless helpful to have a characterization during development and testing as amplifier behavior is most easily understood and analyzed when performance is mapped to a Smith Chart.

Generating a tuner characterization can be a time-consuming effort since every impedance point within the characterization table must be individually tuned to and then measured. Because the precise relationship between the tuner's fundamental parameters and the resulting reflection coefficient (denoted in this paper using $P \rightarrow \Gamma$) may not be understood at the start of the characterization process, the selection of a small set of fundamental parameter settings that provide a given coverage of the Smith Chart is nontrivial. In situations where the behavior of the relationship $P \rightarrow \Gamma$ cannot be easily modelled, manual trial and error can lead to a good distribution of parameter settings that results in the desired characterization. However, an automated approach that is able to determine a sufficient distribution greatly reduces the time required and results in a more consistent result between users.

II. Relationship of Tuner Parameters to Impedance

Traditional load-pull tuners implemented using a slide screw assembly (such as the Maury Microwave Automated Tuner System (ATS) tuner shown in Fig. 1) exhibit a relatively straightforward relationship between fundamental tuner parameters and reflection coefficient [2]. In general, the distance of a mismatch probe from a transmission line (denoted as h in this paper) is able to control the magnitude of the tuner's reflection coefficient $|\Gamma|$ while the position of that probe along the transmission line (denoted as x) is able to control the phase of the reflection coefficient $\angle\Gamma$. That is, the relationship $(h, x) \rightarrow \Gamma$ can be described as:

$$(h, x) \rightarrow \Gamma = \begin{cases} |\Gamma| \propto h \\ \angle\Gamma \propto x \end{cases}.$$

An approximation of this relationship is illustrated in Fig. 2.

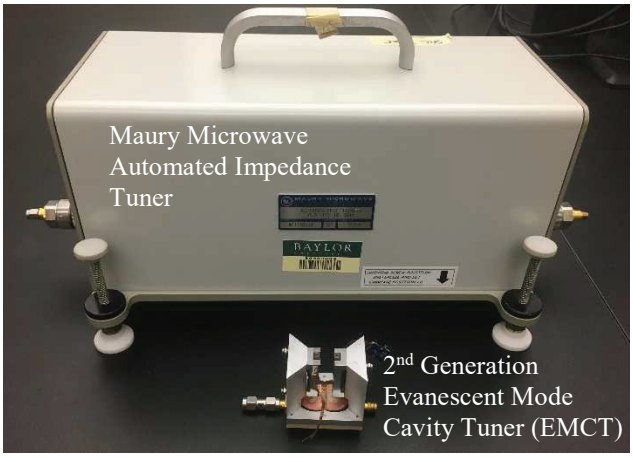

Fig. 1. Impedance tuners characterized in this work are the Maury Microwave ATS tuner (Model MT982B) (top) and the EMCT of Semnani [5] (bottom).

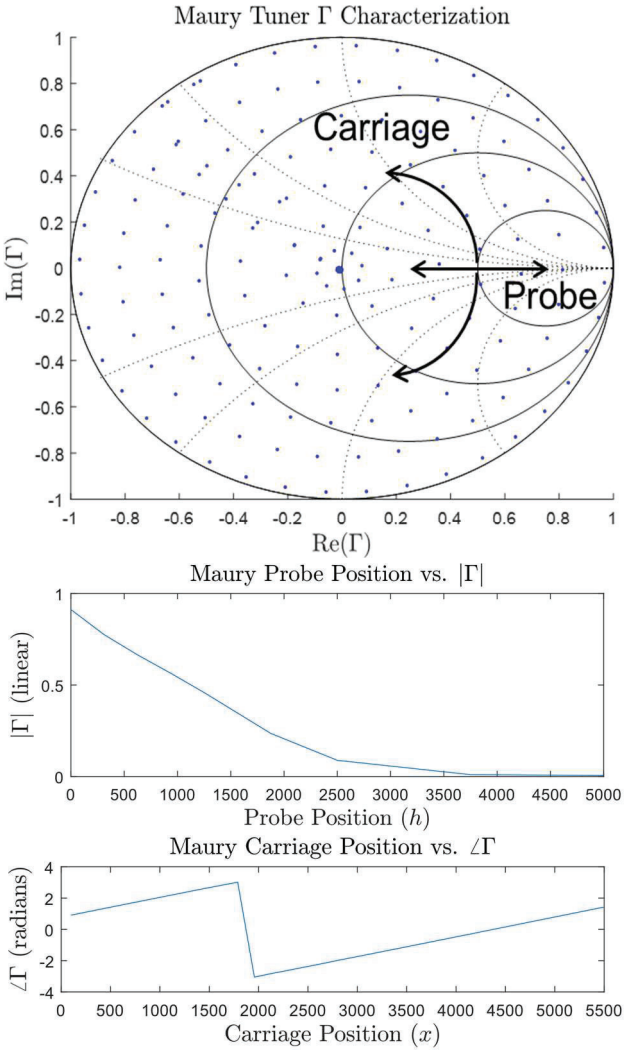

Fig. 2. Illustration of the impact of carriage and probe position within the Maury impedance tuner. In general, the magnitude of the reflection coefficient (line segment in top plot) is controlled by the probe position (middle), and the phase of the reflection coefficient (arc in top plot) is controlled by the carriage position (bottom). In practice, the probe position also impacts the phase by adding a constant phase offset to the carriage position response.

If using a tuner with a more complicated relationship than the previous $(h, x) \rightarrow \Gamma$, these methods are not applicable. In particular, the tuner for which we demonstrate our method, designed by Semnani [4] and later adapted to employ commercial-off-the-shelf actuators [5], utilizes two adjustable evanescent mode resonant cavities. We will refer to this tuner as the evanescent mode cavity tuner (EMCT). This tuner is also shown in Fig. 1. The height of each cavity is adjusted by extending plates attached to linear actuators, whose extension lengths are denoted in 0.5 μm increments as n_1 and n_2. For this device, the input resonant cavity height selects a tuning circle on the Smith Chart with center and radius dependent on the value of n_1, and the output resonant cavity selects a point on this circle dependent on the value of n_2, as illustrated in Fig. 3. As with the slide screw tuner, these relationships are nonlinear, with larger values of (n_1, n_2) resulting in more significant impedance variations. In this situation, the relationship $(n_1, n_2) \rightarrow \Gamma$ cannot be simplified into two independent relationships as was done for $(h, x) \rightarrow \Gamma$.

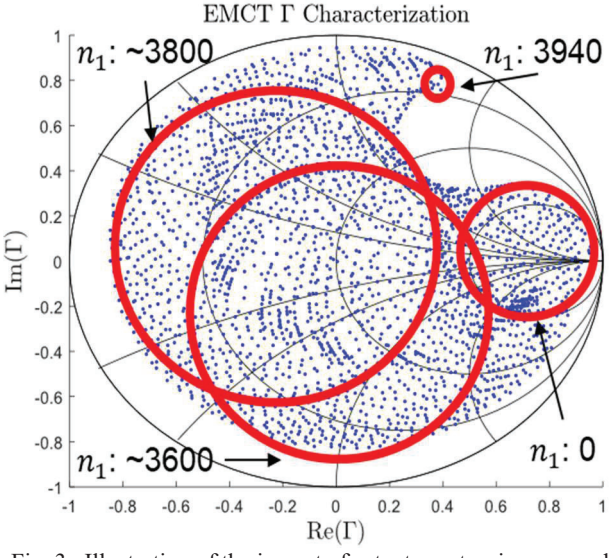

Fig. 3. Illustration of the impact of actuator extensions n_1 and n_2 within the EMCT of [5]. In general, the first actuator (n_1) selects an arc of varying radius and center on the Smith Chart (illustrated with the red circle), while the second actuator (n_2) sweeps along a given arc. In reality, these arcs are not closed and are shown as full circles for illustration purposes.

While a model can be determined by calculating the center and radius of each tuning circle associated with n_1, each circle model would require sweeping n_2, which is complicated by its nonlinear behavior. The approach presented by Spirito [3] could be applied for a fixed value of n_1, but the resulting mapping of n_2 would not be transferrable to other values of n_1. This would allow for the creation of a characterization consisting of points uniformly distributed across the Smith Chart, at the cost of two passes over the fundamental parameter domain.

If uniformity can be sacrificed in favor of ensuring the spacing between points in the final characterization is less than a desired maximum, then a more generic algorithm built upon an interval-halving approach can be used, with fewer restrictions on the nature of the relationship $P \rightarrow \Gamma$. The following section illustrates this algorithm using a tuner with arbitrary parameters $P = (n_1, n_2)$.

III. Recursive Interval-Halving Maximum Separation Algorithm

Let the sorted set of allowed values for the parameters (n_1, n_2) be represented as N_1 and N_2, the Euclidian distance between two values of Γ be represented as $\delta\Gamma$, and the desired maximum point separation be represented as $\Delta\Gamma$. For this discussion, sweeps of n_2 will be performed for each selected value of n_1.

For a given n_2 sweep, start by measuring Γ for the first and last points of the set N_2 and $\delta\Gamma$ between these two points. If this distance is greater than desired maximum point separation $\Delta\Gamma$, then select the next chosen value for n_2 as the midpoint of the set N_2. Note that this has divided the set N_2 into two different intervals: one that runs from the first value of N_2 to the midpoint, and a second from the midpoint to the final value of N_2. Calculate $\delta\Gamma$ for the endpoints of each of these two intervals and divide each interval in half if $\delta\Gamma > \Delta\Gamma$ for each interval. If $\delta\Gamma \leq \Delta\Gamma$ for either of the intervals, then this interval does not need to be halved further. This process can be repeated recursively for each of the new intervals until $\delta\Gamma \leq \Delta\Gamma$ for all intervals, indicating the desired point separation is reached. This process is illustrated in Fig. 4.

Note that this process is not guaranteed to achieve a uniform spacing of points in the resulting characterization, or even within a single parameter sweep. For example, consider the simple example of characterizing the arbitrary one-dimensional function

$$f(x) = e^{\frac{x}{20}}$$

over the domain $0 \leq x \leq 100$ with a desired point separation of no more than 25, as shown in Fig. 5. While a uniformly spaced characterization would contain around 7 points evenly spaced on the y-axis from 0 to 150, the resulting characterization contains 10 points with some intervals sampled beyond the desired density, such as the three points within the range $0 \leq f(x) \leq 25$.

A similar process can be used for the higher-level parameter n_1. Complete the described n_2 sweep process of Fig. 4 for both the first and last points of the set N_1 to create the first n_1 interval. To determine if this interval should be halved, compute $\delta\Gamma$ between the two n_2 sweeps from the N_1 endpoints. This provides a measure of $\delta\Gamma$ between the N_1 endpoints as a function of n_2. For each continuous interval of the n_2 sweeps where the requirement $\delta\Gamma \leq \Delta\Gamma$ is violated, halve the n_1 interval and perform additional sweeps of n_2, with n_2 constrained to the violating interval. This process is illustrated in Fig. 6, and an example subdivision with multiple violating n_2 intervals is illustrated in Fig. 7.

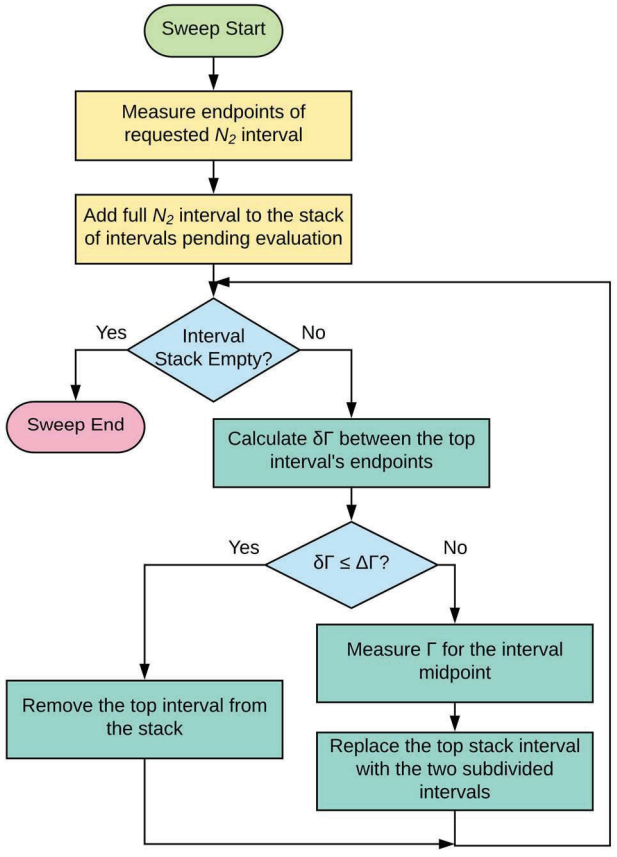

Fig. 4. Flowchart demonstrating recursive interval-halving process for a single parameter.

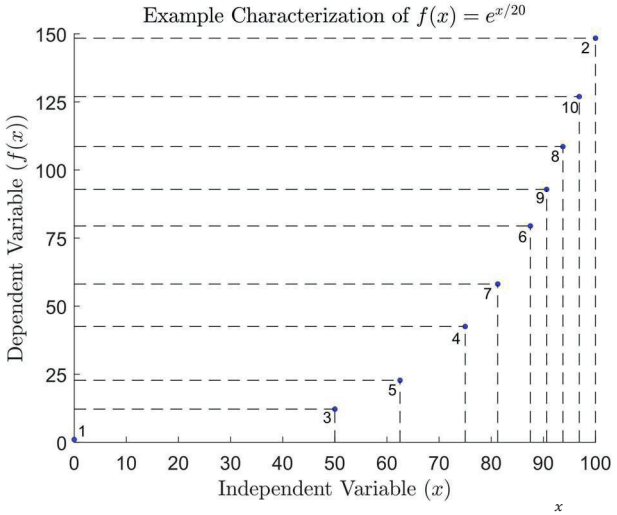

Fig. 5. Example characterization of the function $f(x) = e^{\frac{x}{20}}$ over the domain $0 \leq x \leq 100$ with a desired maximum point separation within the dependent variable space of 25. Each point is numbered in the order that it is evaluated. Note that the separation of points along the y-axis is not uniform, but also does not exceed the desired separation maximum, which is the goal of this characterization algorithm.

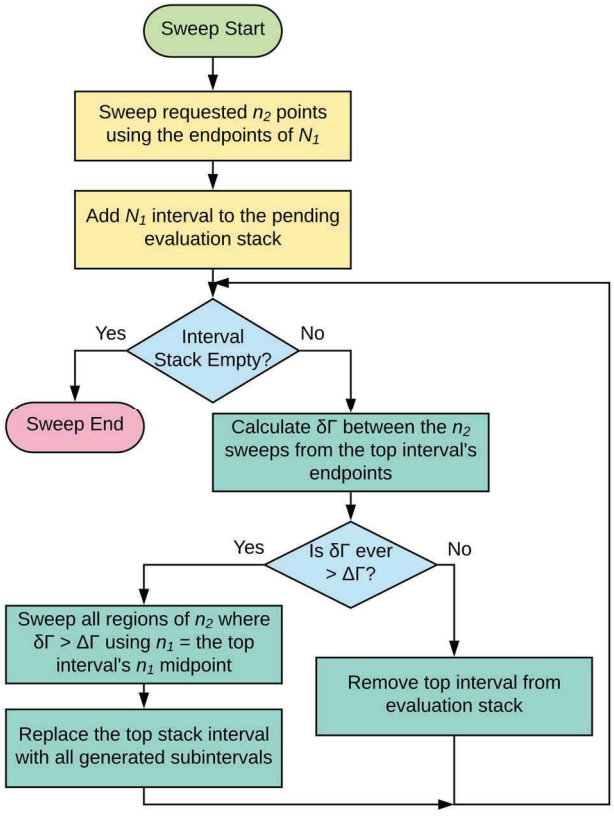

Fig. 6. Flowchart demonstrating the recursive interval-halving process for a second parameter.

IV. Limitations on Tuning Parameter Relationship

While this characterization algorithm functions without generating a model of the underlying relationship between the fundamental parameters and the resulting impedance, there are some constraints that must be maintained to ensure good performance.

First, the relationship $P \rightarrow \Gamma$ is assumed to be smooth—that is, continuous changes in P will result in continuous changes in Γ. Violating this assumption could prevent the interval-halving process from eventually converging. We are unaware of any physically realizable tuner designs that are capable of violating this assumption.

Secondly, it is assumed that the behavior of a given fundamental parameter is such that all resulting values of Γ within a radius ΔΓ correspond to a continuous set of fundamental parameter values. In other words, the parameter sweep should not revisit regions of the Smith Chart that were reached during earlier portions of the sweep. If this assumption is violated, it is possible that the interval-halving process converges sooner than desired. This assumption is actually violated by the EMCT of [5] for the end points of a given n_2 sweep for extreme values of n_1. Compensation for this is accomplished by requiring that a minimum set of points per sweep is visited. If the process converges before this amount, the sweep interval is divided according to a predetermined spacing which ensures the full sweep behavior is observed, and then the interval-halving process is executed with this initial seed of intervals.

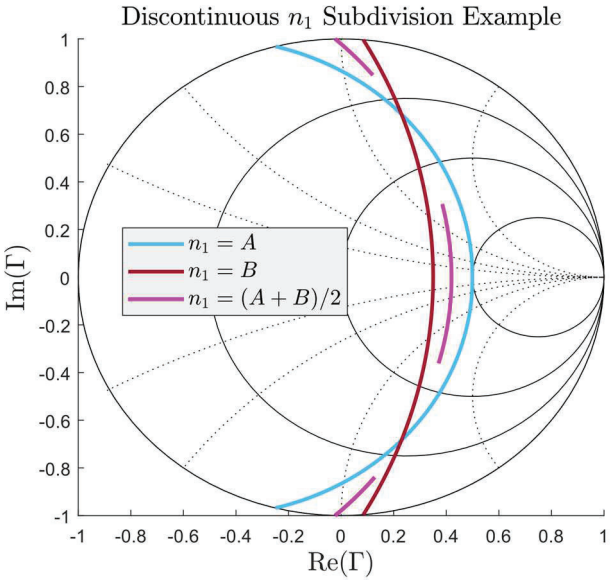

Fig. 7. Example n_1 subdivision with multiple violating N_2 intervals. As n_2 is swept for $n_1 = A$ and $n_2 = B$, $\delta\Gamma \leq \Delta\Gamma$ is violated near the ends of the current N_2 set (mapping to the top and bottom of the Smith Chart) and an additional interval in the middle of the N_2 set (mapping near the vertical center of the Smith Chart). In response, three sweeps of n_2 are made using $n_1 = 0.5(A + B)$ using the three violating intervals of N_2.

Finally, this process is not well suited for a tuner that is controlled using fundamental parameters with a binary functionality, such as the tuner presented by Calabrese [6]. Such a tuner is incompatible with the interval-halving approach as the interval for each parameter is indivisible by nature (each parameter only has two states—no interval halving is possible).

V. Results

An example characterization generated using the approach of Section III with $\Delta\Gamma = 0.1$ and the EMCT of [5] is shown in Fig. 8. The regions of N_1 and N_2 that were sampled more densely during the characterization process are shown in Fig. 9. Note that the spacing in Fig. 9 needed to obtain the characterization of Fig. 8 is extremely irregular and cannot be obtained by any simple linear or exponential sweep.

To achieve the specified ΔΓ, the algorithm visited 971 impedances in 276 seconds, achieving a maximum point separation of 0.08. While this is close to the desired

maximum point separation, the average point separation of 0.03 is much lower. This is because the tuning circles associated with each n_1 value overlap in many instances even for distant values of n_1. As the characterization algorithm only checks for point spacing within a circle and between adjacently selected circles, oversampling can occur along overlapping circles.

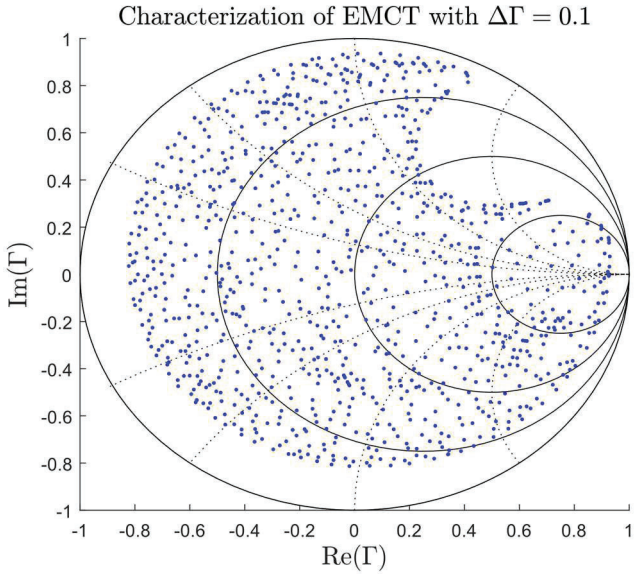

Fig. 8. Characterization of the EMCT [5] generated using the process of Section III with a target point separation of 0.1.

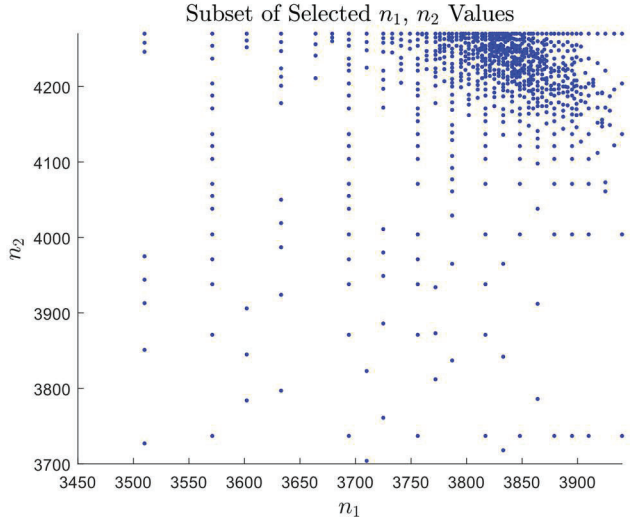

Fig. 9. Subset of the fundamental parameter values chosen during the characterization of Fig. 8. Values of $n_1 < 3450$ and $n_2 < 3700$ are sparsely sampled and excluded from this figure for clarity.

To compare this method with the state of the art, characterizations were performed of the Maury tuner using the same method. Unlike the EMCT, each adjustable component of the Maury tuner requires different amounts of time to set to new positions. As such, it is recommended to use the slower component as the higher-level fundamental parameter n_1. For the Maury tuner, the faster parameter is the probe position, and the slower parameter is the carriage position. To demonstrate, characterizations using either option for n_1 and $\Delta\Gamma = 0.2$ are shown in Figs. 10 and 11 below. These characterizations both provide comparable coverage to that achieved by the Maury software characterization with a target Γ separation of 0.2 shown in Fig 2.

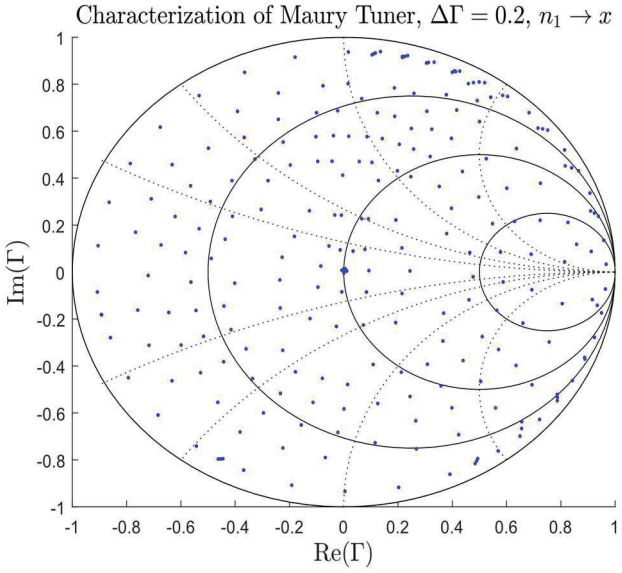

Fig. 10. Characterization of the Maury Tuner generated using the process of Section III with a target point separation of 0.2 and the carriage position as n_1, resulting in a faster characterization process.

Results for each characterization are summarized in Table I. As expected, characterizing the Maury tuner is much faster when the probe position is used as n_2, completing in 67% of the time despite using 46 more measurements. Additionally, our algorithm outperforms the approach built into the Maury tuner's software, evaluating more than twice as many points in 30 fewer seconds.

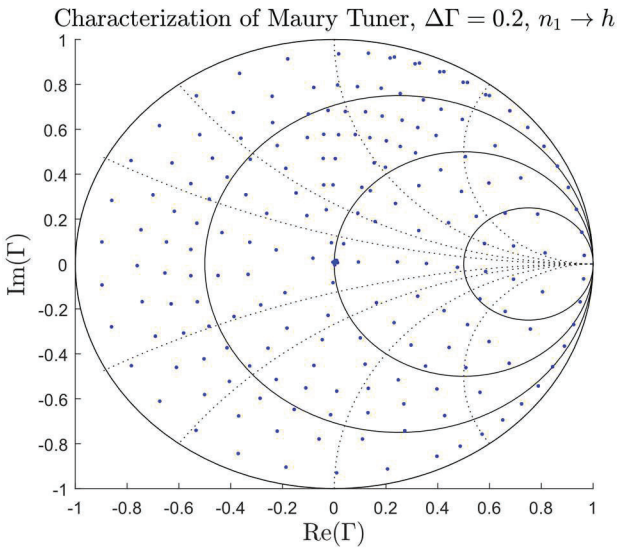

Fig. 11. Characterization of the Maury Tuner generated using the process of Section III with a target point separation of 0.2 and the probe position as n_1, resulting in a slower characterization process.

TABLE I
CHARACTERIZATION PERFORMANCE METRICS

	# of Γ	**Time (s)**	**Min δΓ**	**Max δΓ**	**Avg δΓ**
Maury Software (Fig. 2)	107	800	0.00056	0.1538	0.1226
Maury Fast n_1 (Fig. 10)	250	770	0.00032	0.1763	0.0755
Maury Slow n_1 (Fig. 11)	204	1152	0.00075	0.1673	0.0947
EMCT (Fig. 8)	971	276	0.00005	0.0785	0.0280

VI. CONCLUSION

An efficient approach for choosing tuning parameter values required to achieve a minimum Smith Chart separation in load-pull tuner characterizations has been presented. This characterization approach is expected to be especially useful and efficient in situations where the relationship between fundamental tuning parameters and reflection coefficient is not easily able to be modeled or understood.

ACKNOWLEDGEMENT

This research was funded by the Army Research Laboratory (Grant No. W911NF-16-2-0054). The views and opinions expressed do not necessarily represent the opinions of the U.S. Government.

REFERENCES

[1] Z. Hays *et al*., "Fast impedance matching using interval halving of resonator position numbers for a high-power evanescent-mode cavity tuner," *2018 IEEE Radio and Wireless Symposium (RWS)*, Anaheim, CA, 2018, pp. 256-258.

[2] G.R. Simpson, *Methods for calibrating an impedance tuner, for conducting load pull measurements, and for measuring data for noise parameters*. (2014, Oct. 25). *US9632124B2*. Accessed on: July 17, 2019. [Online]. Available: https://patents.google.com/patent/US9632124B2/

[3] M. Spirito *et al*., "A Novel Method for Characterizing RF Automated Tuners," *58th ARFTG Conference Digest*, San Diego, CA, USA, 2001, pp. 1-6.

[4] A. Semnani, M. Abu Khater, Y.-C. Wu, and D. Peroulis, "An Electronically-Tunable High-Power Impedance Tuner with Integrated Closed-Loop Control," *IEEE Microwave and Wireless Components Letters*, Vol. 27, No. 8, August 2017, pp. 754-756.

[5] A. Semnani, G.S. Shaffer, M.D. Sinanis, and D. Peroulis, "High-Power Impedance Tuner Utilising Substrate-Integrated Evanescent-Mode Cavity Technology and External Linear Actuators," *IET Microwaves, Antennas & Propagation*, Vol. 13, No. 12, 2019, pp. 2067-2072.

[6] C. Calabrese *et al*., "Fast Switched-Stub Impedance Tuner Reconfiguration for Frequency and Beam Agile Radar and Electronic Warfare Applications," *2020 IEEE International Radar Conference (RADAR)*, Washington, DC, USA, 2020, pp. 94-98, doi: 10.1109/RADAR42522.2020.9114834